

## CALCULATION OF ELECTRONIC PROPERTIES AND FORMATION ENERGY OF NANOSTRUCTURE OF OXIDES $\text{Li}_2\text{O}$ , $\text{B}_2\text{O}_3$ AND $\text{Y}_2\text{O}_3$

M.M. ASADOV<sup>1,2</sup>, E.S. KULI-ZADE<sup>1</sup>, S.N. MUSTAFAEVA<sup>3</sup>

<sup>1</sup>*Institute of Catalysis and Inorganic Chemistry. Ministry of Science and Education Azerbaijan. Baku*

<sup>2</sup>*Azerbaijan State Oil and Industry University, SRI GPOGC. Azerbaijan. Baku*

<sup>3</sup>*Institute of Physics. Ministry of Science and Education Azerbaijan. Baku*

*E-mail: solmust@gmail.com; mirasadov@gmail.com*

The previous physicochemical descriptions of the boundary systems of the  $\text{Li}_2\text{O} - \text{B}_2\text{O}_3 - \text{Y}_2\text{O}_3$  quasi-ternary system have been modified taking into account the literature data and our experimental results. The nature of the physicochemical interaction of quasibinary  $\text{Li}_2\text{O} - \text{B}_2\text{O}_3$ ,  $\text{Y}_2\text{O}_3 - \text{B}_2\text{O}_3$ ,  $\text{Li}_2\text{O} - \text{Y}_2\text{O}_3$  systems and the properties of their components ( $\text{Li}_2\text{O}$ ,  $\text{B}_2\text{O}_3$  и  $\text{Y}_2\text{O}_3$ ) were optimized using the electronic structure calculation data from this work. Based on the optimized properties  $\text{Li}_2\text{O}$ ,  $\text{B}_2\text{O}_3$  and  $\text{Y}_2\text{O}_3$ , a comparison with experimental data was made. The agreement between calculated and experimental data is improved. The initial configurations of lithium, boron and yttrium oxides ( $\text{Li}_2\text{O}$ ,  $\text{B}_2\text{O}_3$ ,  $\text{Y}_2\text{O}_3$ ) were calculated by taking into account the optimized crystal structure of these compounds with density functional theory. The structures of lithium and yttrium oxides ( $\text{Li}_2\text{O}$ ,  $\text{Y}_2\text{O}_3$ ) are accepted as a cubic system, and for boron oxide ( $\text{B}_2\text{O}_3$ ), as a trigonal system. DFT calculated the electronic properties of these compounds, which are compared with the results of existing studies. Densities of electronic states (DOS) and energy gap HOMO-LUMO of these oxides are analyzed. Taking into account the fact that the ionization energy of the atomic orbitals of oxides differ greatly from each other, the effects of the s-, p-, and d-states on the chemical bond in  $\text{Li}_2\text{O}$ ,  $\text{B}_2\text{O}_3$ ,  $\text{Y}_2\text{O}_3$  compounds are analyzed. The calculated values of the formation energy of  $\text{Li}_2\text{O}$ ,  $\text{B}_2\text{O}_3$ ,  $\text{Y}_2\text{O}_3$  compounds, as well as their melting temperatures, are compared with known data. The change in the enthalpy of formation of these oxides does not correlate with an increase in their melting point.

**Keywords:** nanostructure of oxides  $\text{Li}_2\text{O}$ ,  $\text{B}_2\text{O}_3$ ,  $\text{Y}_2\text{O}_3$ , density functional theory (DFT), DFT calculation, density of electronic states (DOS), formation energy.

**PACS:** 61.72.-y; 71.20.Nr; 72.20.-i

### 1. INTRODUCTION

Oxide materials are used in nano and optoelectronics. For example, they will be used for the manufacture of lasers, storage of solar panels, optical detectors, waveguides. Materials based on oxide glasses make it possible to fabricate samples of a given size and shape [1–3]. Materials containing  $\text{Li}_2\text{O}$  (modifier) and  $\text{B}_2\text{O}_3$  (glass former) have ionic conductivity. For example, lithium borate glasses containing lithium ions are used in solid state batteries with a high charge density [4, 5]. Ions of rare earth elements (REE), in particular,  $\text{Y}_2\text{O}_3$ , can change the properties of boron oxide and lithium [6]. The resulting glassy materials can be slowly transformed into a crystalline state. When REE are introduced into oxide compounds, REE electrons pass from the low-valence state to the excited high-valence state. In this case, the properties of the material change, for example, the refractive index, band gap, and laser gain increase [7]. The electrical conductivity of oxide glasses can decrease with an increase in the concentration of introduced rare earth elements [8].

Phase equilibria of binary boundary systems  $\text{Li}_2\text{O} - \text{B}_2\text{O}_3$ ,  $\text{Y}_2\text{O}_3 - \text{B}_2\text{O}_3$ ,  $\text{Li}_2\text{O} - \text{Y}_2\text{O}_3$  were studied by methods of physicochemical and thermodynamic analyzes [1-3]. The electronic properties of binary oxides  $\text{Li}_2\text{O}$  [9-11],  $\text{Y}_2\text{O}_3$  [12,13] and  $\text{B}_2\text{O}_3$  [14-18] have been studied: band structure, electronic density of states, atomic and electronic structure of crystals. The experimentally found and model calculated enthalpies of formation of these

compounds are also known [19–22]. The purpose of this work is to improve the agreement between the known and our calculated and experimental data of  $\text{Li}_2\text{O} - \text{B}_2\text{O}_3$ ,  $\text{Y}_2\text{O}_3 - \text{B}_2\text{O}_3$ ,  $\text{Li}_2\text{O} - \text{Y}_2\text{O}_3$  systems based on the optimized properties of the components ( $\text{Li}_2\text{O}$ ,  $\text{B}_2\text{O}_3$ ,  $\text{Y}_2\text{O}_3$ ). In addition to the above, the calculation of the electronic properties and enthalpies of formation of oxides ( $\text{Li}_2\text{O}$ ,  $\text{B}_2\text{O}_3$ ,  $\text{Y}_2\text{O}_3$ ) in the framework of the theory of electron density of states.

### 2. METHOD OF CALCULATIONS AND EXPERIMENT

*DFT calculation.* The band structure and density of electronic states were calculated based on the density functional theory (DFT) using a quantum chemical software package [23]. The atoms in the ground state contained in binary components ( $\text{Li}_2\text{O}$ ,  $\text{B}_2\text{O}_3$ ,  $\text{Y}_2\text{O}_3$ ) were considered as the initial electronic configurations. Supercells containing oxide components of the  $\text{Li}_2\text{O} - \text{Y}_2\text{O}_3 - \text{B}_2\text{O}_3$  system were used. In DFT calculations of the properties of compounds, the effects of exchange and correlation in the total energy of the system were taken into account in the framework of the generalized gradient approximation (GGA) according to the Perdew–Burke–Ernzerhof (PBE) scheme [24, 25]. The energy change was calculated for the basis set, taking into account the valence s-, p-, and d-orbitals of the component atoms.

The geometry of the unit cells  $\text{Li}_2\text{O}$ ,  $\text{B}_2\text{O}_3$  and  $\text{Y}_2\text{O}_3$  was optimized. When calculating the self-consistent field, the basis was constructed using plane

waves with a kinetic energy  $\leq 300$  eV. In calculations, the wave cutoff energy was chosen such that the convergence in the total energy of the unit cell was  $\geq 5 \times 10^{-6}$  eV/atom. The convergence threshold for interatomic forces was  $10^{-4}$  eV/Å. The choice of k-points of the reciprocal lattice in the Brillouin zone was carried out using the Monkhorst–Pack method [26]. To subdivide the Brillouin zone, a  $2 \times 2 \times 2$  k-grid was used. This choice of values ensures high accuracy in calculating the supercell parameters of the compounds.

The optimized unit cell parameters of binary oxides were used in the calculations. The energy of formation ( $E_f$ ) (or the enthalpy  $\Delta_f H^0$  of formation) of the compounds was calculated at zero temperature using a similar formula [27]. For example, for the  $\text{Li}_2\text{O}$  compound, the value of  $E_f$  was calculated using the equation:

$$E_f = \left(\frac{1}{2}\right) [E_{\text{Li}_2\text{O}}^{\text{total}} - (2E_{\text{Li}} + E_{\text{O}})] \quad (1)$$

where  $E_{\text{Li}_2\text{O}}^{\text{total}}$  total is the total unit cell energy of the  $\text{Li}_2\text{O}$  compound (per formula unit),  $E_{\text{Li}}$  and  $E_{\text{O}}$  are the energies of the elements Li and O (per atom), respectively.

*Sample preparation and experimental procedure.* Samples for refinement of phase diagrams and equilibria in the  $\text{Li}_2\text{O} - \text{Y}_2\text{O}_3 - \text{B}_2\text{O}_3$  system were synthesized from the following starting materials:  $\text{Li}_2\text{CO}_3$  (chemically pure),  $\text{H}_3\text{BO}_3$  (OSCh 12-13), and

$\text{Y}_2\text{O}_3$  with a purity of 99.99%. Synthesis of samples of the system was carried out according to the procedure described in [1]. The synthesized samples were identified by methods of physico-chemical analysis (PCA), X-ray diffractometry (XRD; DRON-2 diffractometer,  $\text{CuK}\alpha$  radiation) and differential thermal analysis (DTA; Jupiter STA 449 Netzsch).

### 3. RESULTS AND DISCUSSION

*Lithium oxide*  $\text{Li}_2\text{O}$  at atmospheric pressure and room temperature has a cubic antiferroite structure ( $\text{CaF}_2$ -type) with parameter  $a_0 = 4.610$  Å, space group  $Fm\bar{3}m$  (No 225),  $Z = 4$ . Due to deformation of the cubic phase,  $\alpha - \text{Li}_2\text{O}$ , a rhombohedral phase ( $Rm\bar{3}H$ ) is formed, which coexists with it,  $\alpha = 90.16^\circ$ . DFT GGA-PBE calculations of the lattice parameter ( $a_0 = 4.57$  Å), band structure, and density of electronic states (DOS) of the  $\alpha - \text{Li}_2\text{O}$  compound are in good agreement with other calculated [9,10] data. The calculated band gap  $E_g = 5.39$  eV  $\alpha - \text{Li}_2\text{O}$  is smaller than the experimental data  $E_g$  (Table 1).

Structural, electronic properties, and enthalpies of formation of  $\alpha - \text{Li}_2\text{O}$  binary oxides were studied using DFT GGA-PBE. The calculated properties for  $\alpha - \text{Li}_2\text{O}$  agree well with calculated and experimental data [9]. The direct band gap of the  $\alpha - \text{Li}_2\text{O}$  phase is 5.1 eV. The total density of states TDOS  $\alpha - \text{Li}_2\text{O}$  and the partial densities of states PDOS Li and O are shown in Fig. 1.

Table 1.

Crystal	$a, \text{Å}$	$E_g, \text{eV}$
$\alpha - \text{Li}_2\text{O}$	4.533, 4.631 [9], 4.573 [10]	5.1, 5.39 [9], 5.5 [10], 5 [28]

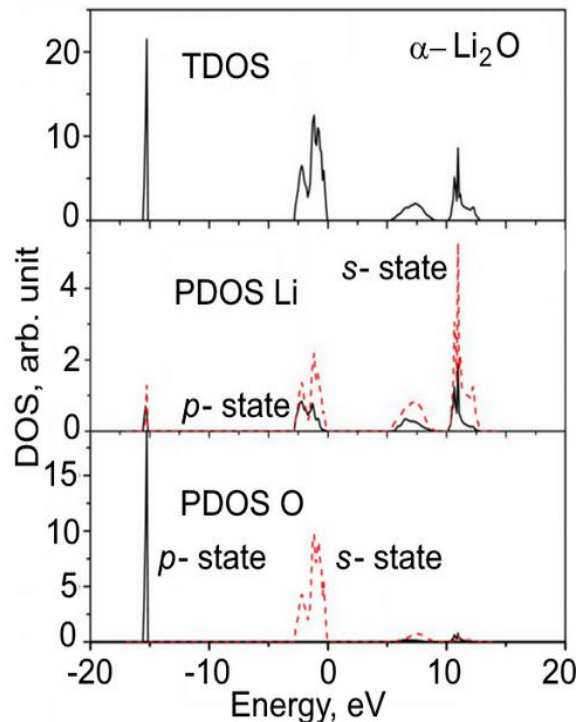


Fig. 1. Total (DOS) and partial (PDOS) electron densities of states for the cubic phase of  $\alpha - \text{Li}_2\text{O}$ .

The shape of the PDOS of the Li and O atoms differ from each other because their electronic configurations are different. The theoretically calculated ionization energies of atomic orbitals of chemical elements [29] also differ from each other. The calculated ionization energies of the orbitals of Li and O atoms are: for Li, the 2s state (5.3 eV), for O, the 2s state (28.5 eV), and the 2p state (7.1 eV). Figure 2 shows that Li s-orbitals and O p-orbitals have a relatively large contribution to the total electron density of the system.

*Yttrium oxide*  $Y_2O_3$ . For the crystal structure of  $Y_2O_3$ , three polymorphic modifications are known: cubic C-type ( $\alpha - Y_2O_3$ ), monoclinic (B-type) and hexagonal H-type ( $H - Y_2O_3$ ) systems [1]. The  $\alpha - Y_2O_3$  (space group  $Ia\bar{3}$  (No 206);  $a = 10.60 \text{ \AA}$ ,  $\beta = 90^\circ$ ) structure transforms into the high-temperature form  $H - Y_2O_3$  at a temperature  $\sim 2700 \text{ K}$ , [1]. This  $H - Y_2O_3$  structure has a hexagonal syngony (space group  $P3m1$  (No 164)).

For the  $Y_2O_3$  compound, the following data are given in early sources of information [30-33]. The B-type has a monoclinic structure (space group  $C2m$ ) with lattice constants:  $a = 13.91$ ,  $b = 3.483$ ,  $c = 8.093 \text{ \AA}$ ,  $\beta = 100.15^\circ$ . Phase transition temperature  $T = 1380 \text{ K}$ , enthalpy  $\Delta H_{tr(C-B)} = 310 \text{ cal/mol}$ , and entropy  $\Delta S_{tr(C-B)} = 0.24 \text{ cal/(mol} \cdot ^\circ\text{C)}$ . The existence of a hexagonal H-type with lattice constants at  $2653 \text{ K}$  is also reported:  $2600 \pm 30 \text{ K}$  phase transition has an enthalpy  $\Delta H_{tr(B-H)} = 6000 \pm 2000 \text{ cal/mol}$ . A melting temperature of  $T_m = 2700 \pm 10 \text{ K}$  and an enthalpy of melting  $\Delta H_m = 20000 \pm 2000 \text{ cal/mol}$  were proposed [30].

Low-temperature modification  $\alpha - Y_2O_3$  ( $CaF_2$ -type, or  $Mn_2O_3$ ; space group  $Ia\bar{3}$  (No 206)) with cell parameter  $a = 10.605\text{--}10.640 \text{ \AA}$ ,  $Z = 4$  [31]. The structure of the  $\alpha - Y_2O_3$  crystal is analogous to the unit cell of fluorite, in which part of the anion is missing.  $\alpha - Y_2O_3$  is an insulator under room conditions, with a direct band gap of  $4.54\text{--}5.5 \text{ eV}$ , located at point  $\Gamma$  in reciprocal space.

Various thermodynamic data are known for the  $Y_2O_3$  phase transition temperature [32]. The following values are given for the C  $\rightarrow$  B phase transition:  $\Delta H_{C \rightarrow B} = 12.833 \text{ kJ/mol}$ ;  $\Delta S_{C \rightarrow B} = 4.080 \text{ J/(mol}\cdot\text{K)}$ . A for the C  $\rightarrow$  H phase transition, on average, the following values are given:  $\Delta H_{C \rightarrow H} = 36.25 \pm 5.75 \text{ kJ/mol}$ ;  $\Delta S_{C \rightarrow H} = 14.1 \text{ J/(mol}\cdot\text{K)}$ . For the phase transition (C  $\rightarrow$  H) is given on average  $T_{C \rightarrow H} = 2590 \pm 18 \text{ K}$ . And for the melting point  $Y_2O_3$  is known  $T_m = 2590 \pm 18 \text{ K}$ .

For the monoclinic structure  $Y_2O_3$  (B-type; space group  $C2m$ ) different authors give lattice parameters that vary in the following intervals:  $a = 13.871\text{--}14.060 \text{ \AA}$ ,  $b = 3.4487\text{--}3.5360 \text{ \AA}$ ,  $c = 8.567\text{--}8.629 \text{ \AA}$ ,  $\beta = 100\text{--}100.12^\circ$  [33].

The results of calculations of the total density of states (DOS) and partial DOS (PDOS) for the Y and O atoms of the  $\alpha - Y_2O_3$  compound show the following. The nature of the spectra of total DOS and partial PDOS for  $\alpha - Y_2O_3$  corresponds to the spectra of the low-energy configuration. The same energy spectra are characteristic of the  $Y_6O_9$  cluster [12].

The Y-4s states lie at low energies and are not visible in Fig. 3. The Y-4p states are observed in the lower energy part of the spectra. The 2s orbitals of oxygen atoms predominate in the middle energy part of the spectra.

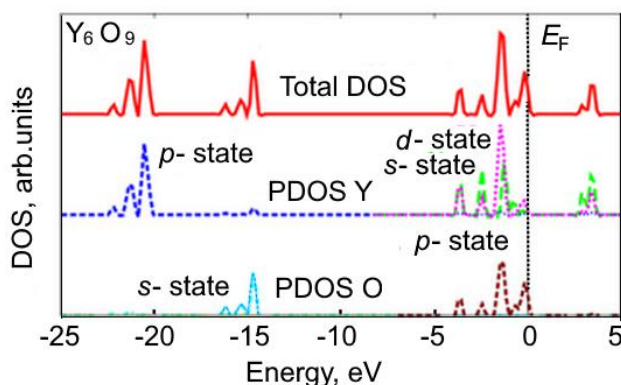


Fig. 2. Total (DOS) and partial (PDOS) electron densities of states for the  $Y_6O_9$  cluster.

The formation of molecular orbitals (MO), taking into account the hybridization of electron orbitals, can explain the formation of  $Y^{3+}$  ions. When distributing electrons over MO atoms  $\alpha - Y_2O_3$  in accordance with the principles of distribution, the last electrons must occupy unfilled orbitals, one electron per orbital. Therefore, the presence of unpaired electrons on MO imparts new properties to the  $\alpha - Y_2O_3$  molecule.

In the HOMO-LUMO theory of molecular orbitals, the gap is the energy gap between the highest

occupied molecular orbital (HOMO) and the lowest vacant molecular orbital (LUMO). The HOMO-LUMO gap is an important parameter of nanostructures and can serve as an analogue of the band gap for nanotubes. States near the HOMO level (Fig. 3) consist of hybridized 5s and 4d states of Y atoms along with O-2p states. The 4d electrons of Y atoms make a significant contribution to interatomic bonds. In the HOMO band structure, the  $\alpha - Y_2O_3$  level mainly consists of O-2p orbitals. And LUMO energy  $\alpha - Y_2O_3$  is mainly composed of Y-5s orbitals.

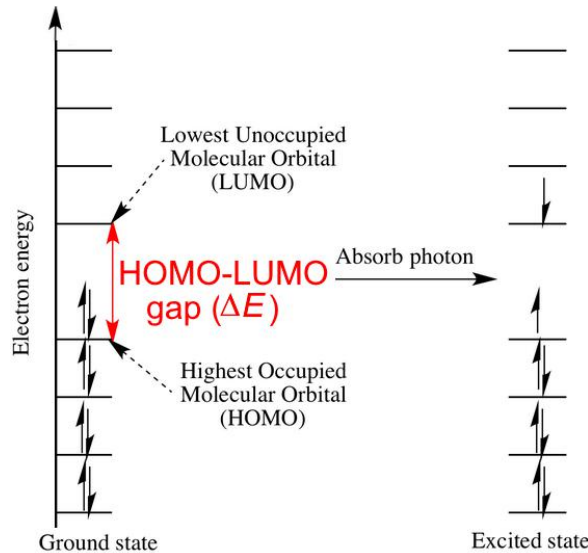


Fig. 3. Diagram of the HOMO-LUMO gap of the optical spectrum.

The calculated ionization energies of the orbitals of the Y and O atoms are [29]: for Y the 5s state (5.3 eV), the 4d state (5.6 eV), for O the 2s state (28.5 eV), the 2p state (7.1 eV).

*Boron oxide*  $B_2O_3$  has two polymorphs (trigonal  $\alpha - B_2O_3$  and orthorhombic  $\beta - B_2O_3$  systems). with different coordination numbers of boron atoms [14–16]. At room temperature and normal pressure, the low-temperature modification  $\alpha - B_2O_3$  has a trigonal structure.  $\alpha - B_2O_3$  is characterized with a three-dimensional grid formed from triangles of  $BO_3$  structural units.  $\alpha - B_2O_3$  with lattice parameters  $a = 4.35 \text{ \AA}$ ,  $c = 8.39 \text{ \AA}$  belongs to the space group  $P3/121$

(№ 152) [15]. At high pressure, the orthorhombic modification ( $\beta - B_2O_3$ ) is stable. It consists of a framework of linked  $BO_4$  tetrahedra [16].

Crystalline  $\alpha - B_2O_3$  is a wide-gap insulator. The calculated band gap is about 9 eV. This corresponds to the known values of 9.1 eV [7, 17].

Densities of states (PDOS) of oxygen and boron crystal  $\alpha - B_2O_3$  (Figure 4) indicate the following. The valence band is primarily made up of oxygen 2p orbitals, while the bottom of the conduction band is made up primarily of boron orbitals. The PDOS of the (101) surface of the  $\alpha - B_2O_3$  compound [18] is also characterized by such an electron density distribution.

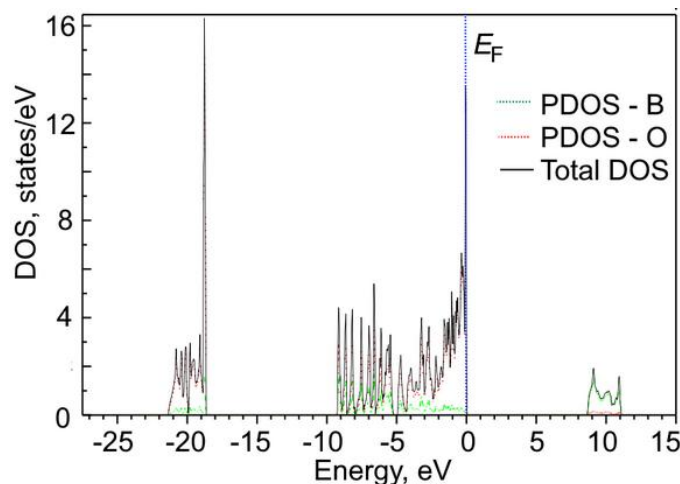


Fig. 4. Total (DOS) and partial (PDOS) electron densities of states for  $\alpha - B_2O_3$ .

The calculated ionization energies of the orbitals of the B and O atoms are [29]: for B, the 2s-state (12.6 eV), 2p-state (6.7 eV), for O, the 2s-state (28.5 eV), 2p-state (7.1 eV).

*Enthalpy of formation.* In calculating the energy of formation of  $Li_2O$ ,  $Y_2O_3$ ,  $B_2O_3$  the standard states of the elements Li, Y, B, and O at 298.15 K were used.

DFT GGA-PBE the enthalpy of formation ( $E_f \approx \Delta_f H^0$ )  $Li_2O$ ,  $Y_2O_3$ ,  $B_2O_3$  calculated by us at  $T = 0 \text{ K}$  is given in Table. 2. Comparison of the calculated values of  $\Delta_f H^0$  with the known data [1, 19–22] of compounds  $Li_2O$ ,  $Y_2O_3$ ,  $B_2O_3$  indicates a small spread between the values of  $\Delta_f H^0$  (Table 2).

DFT GGA-PBE calculated enthalpy of formation of compounds  $\text{Li}_2\text{O}$ ,  $\text{B}_2\text{O}_3$ ,  $\text{Y}_2\text{O}_3$ 

Compound (solid)	$-E_f$ , calc eV / atom	$-\Delta_f H^0$ , calc kJ / mol	$-\Delta_f H_{298}^0$ , kJ / mol [1, 19-22]	$T_m$ , K [1]
$\text{Li}_2\text{O}$	1.99	596	598	1711
$\text{B}_2\text{O}_3$	2.56	1235	1273	753
$\text{Y}_2\text{O}_3$	3.85	1856	1905	2698

From the point of view of the development of functional materials with the participation of binary oxides  $\text{Li}_2\text{O}$ ,  $\text{B}_2\text{O}_3$ ,  $\text{Y}_2\text{O}_3$  data on phase equilibria and structural-phase states in a multicomponent system  $\text{Li}_2\text{O} - \text{B}_2\text{O}_3 - \text{Y}_2\text{O}_3$  are of interest. Some ternary oxide compounds in the  $\text{Li}_2\text{O} - \text{B}_2\text{O}_3 - \text{Y}_2\text{O}_3$  system exhibit lattice instability in different temperature ranges. These unstable structural-phase states of the crystal lattice manifest themselves in the features on the temperature dependences of the physicochemical and mechanical properties. Transition states are difficult to study experimentally. Therefore, theoretical studies are needed according to the forecast of regularities taking into account structural data.

Taking into account the stability limits of ternary compounds in a  $\text{Li}_2\text{O} - \text{B}_2\text{O}_3 - \text{Y}_2\text{O}_3$  quasi-ternary system, we have established phase boundaries between compounds with different stoichiometric compositions.

Equilibrium phase regularities in boundary  $\text{Li}_2\text{O} - \text{B}_2\text{O}_3$ ,  $\text{Y}_2\text{O}_3 - \text{B}_2\text{O}_3$ ,  $\text{Li}_2\text{O} - \text{Y}_2\text{O}_3$  quasi-binary systems are established on the basis of PCA and analysis of crystal parameters. This approach made it possible to reveal inconsistencies between known data, typical and special stoichiometric compositions, and phase boundaries in  $T - x$  phase diagrams.

The formation of stoichiometric compositions of triple oxides, in particular, is determined by geometric factors: the desire of the crystal system to completely fill the structural space, to the highest symmetry and to create the maximum possible number of "bonds" between atoms. Based on the synthesized samples, we refined the  $T-x$  phase diagrams of  $\text{Li}_2\text{O} - \text{B}_2\text{O}_3$ ,  $\text{Y}_2\text{O}_3 - \text{B}_2\text{O}_3$ ,  $\text{Li}_2\text{O} - \text{Y}_2\text{O}_3$  systems (Figs. 5a-d). The analysis shows that the agreement between the known and our calculated and experimental data on these systems is improved.

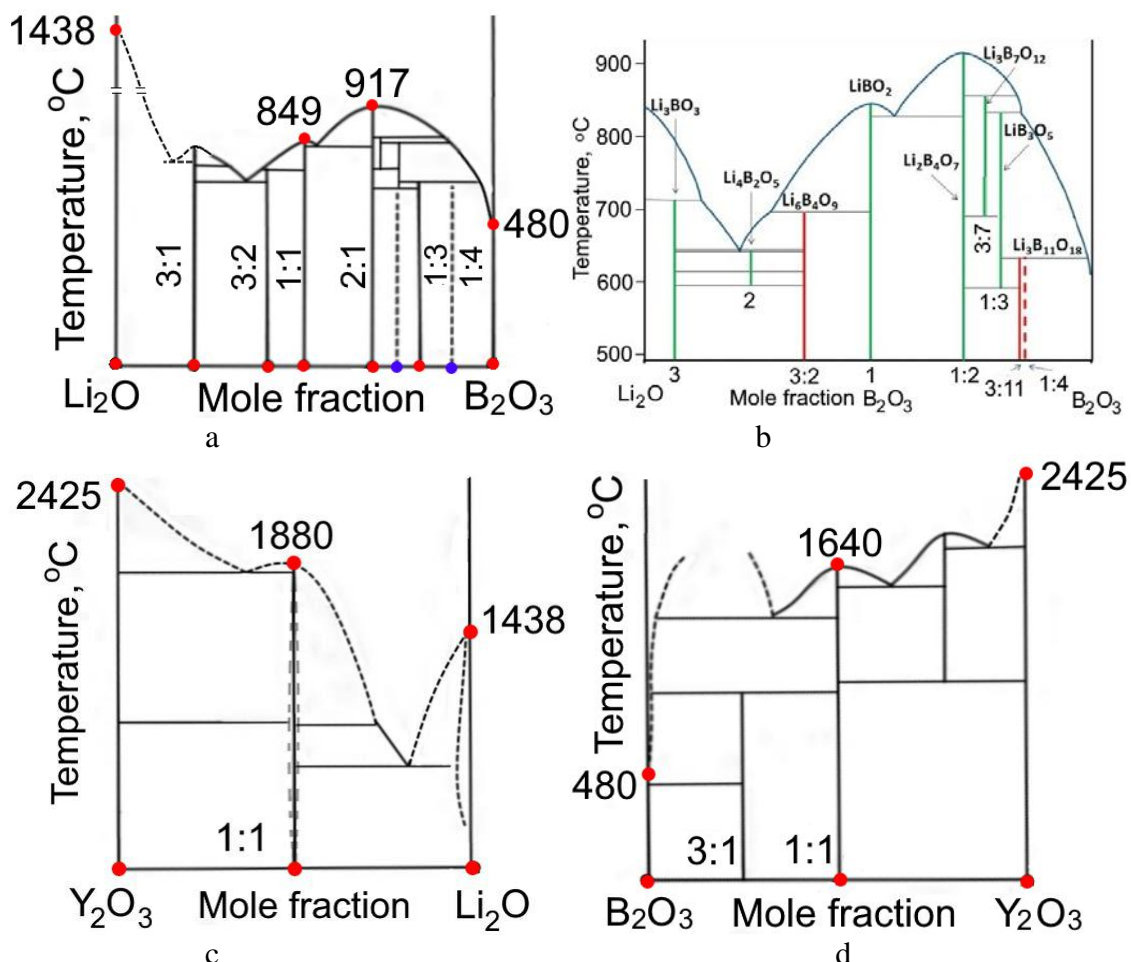


Fig. 5.  $T - x$  phase diagrams of systems:  $\text{Li}_2\text{O} - \text{B}_2\text{O}_3$  (a) [1],  $\text{Li}_2\text{O} - \text{B}_2\text{O}_3$  (b) [34],  $\text{Li}_2\text{O} - \text{Y}_2\text{O}_3$  (c),  $\text{Y}_2\text{O}_3 - \text{B}_2\text{O}_3$  (d).



The conditions for the formation and stability of crystal structures depend on the ratio and combination of the geometric parameters of atoms and their electronic structure. As can be seen from Figs. 5a-d, in the systems  $\text{Li}_2\text{O} - \text{B}_2\text{O}_3$ ,  $\text{Y}_2\text{O}_3 - \text{B}_2\text{O}_3$ ,  $\text{Li}_2\text{O} - \text{Y}_2\text{O}_3$ , a different number of ternary compounds with a three-dimensional periodic structure with different systems are formed. In crystal lattices, in which atoms are arranged in strictly fixed positions.

For binary A-B systems, the use of such characteristics as, for example, the size factor (ratio of element radii  $r_A/r_B$  or  $\delta = 1 - r_A/r_B$ ) seems to be ineffective for determining structural features. To determine the stability limits of crystal structures of different syngonies, in addition to the influence of the size factor on the stability of compounds, modern calculation methods are also used. This is due to the fact that the stability of crystal structures of different syngonies depends on many factors (for example, the electronic structure), which must be taken into account when determining the stability of structural-phase states. Below, we consider the results of calculations of the electronic properties and enthalpy of formation of oxides  $\text{Li}_2\text{O}$ ,  $\text{B}_2\text{O}_3$ ,  $\text{Y}_2\text{O}_3$  in the framework of the theory of electron density of states.

## CONCLUSIONS

The initial supercell configurations of  $\text{Li}_2\text{O}$ ,  $\text{B}_2\text{O}_3$ ,  $\text{Y}_2\text{O}_3$  oxide crystals were optimized and the structures were calculated using the density functional theory. The spectra of the density of states reflect the regularities of the influence of the atomic orbitals of oxygen, lithium, boron and yttrium on the chemical bond in the compounds  $\text{Li}_2\text{O}$ ,  $\text{B}_2\text{O}_3$ ,  $\text{Y}_2\text{O}_3$ .

The formation of ions in these oxides, as in other crystalline compounds, is explained by the formation of

molecular orbitals (MOs), taking into account the hybridization of electron orbitals. When distributing electrons over MO atoms of a compound, in accordance with the principles of distribution, the last electrons must occupy orbitals, one electron per orbital. Therefore, the presence of unpaired electrons on the MO imparts new properties to the substance molecule. In the  $\alpha - \text{Y}_2\text{O}_3$  crystal the orbitals of the valence bond, in particular, the oxygen atom ( $2p^4$ ) are less than half filled, and the valence orbital of the yttrium atom ( $5s^2$ ) is filled. Then the probability of filling the  $2p^4$  orbital of oxygen with electrons  $\alpha - \text{Y}_2\text{O}_3$  is greater than the filling of the  $5s^2$  orbital Y. The main contribution to the  $2s$ -,  $2p$ -states of oxygen is associated with low-energy molecular orbitals, including the corresponding atomic orbitals of lithium ( $1s$ -,  $2s$ -states), boron ( $1s$ -,  $2s$ -,  $2p$ -states) and yttrium ( $5s$ -,  $4d$ - states).

The change in the enthalpy of formation of these oxides does not correlate with an increase in their melting points. For the formation energy of  $\text{Li}_2\text{O}$ ,  $\text{B}_2\text{O}_3$ ,  $\text{Y}_2\text{O}_3$  compounds, the following values were obtained ( $-E_f$ , eV / atom): 1.99, 2.56 and 3.85 eV/atom, respectively.

## ACKNOWLEDGMENTS

The work has been partially funded by from the Science Development Foundation with the President of the Republic of Azerbaijan (EIF) (grant No EIF-BGM-3-BRFTF-2+/2017-15/05/1-M-13) and the Russian Foundation for Basic Research (RFBR) (project № Az a2018).

## CONFLICT OF INTEREST

The authors declare that they have no conflict of interest.

- [1] M.M. Asadov, E.S. Kuli-zade. J. Alloys Compd. 2020. V. 842. P. 155632. <https://doi.org/10.1016/j.jallcom.2020.155632>
- [2] M.M. Asadov, N.A. Akhmedova. Russ. J. Inorg. Chem. 2020. V. 65. № 7. P. 1061. <https://doi.org/10.1134/S0036023620070013>
- [3] M.M. Asadov, N.A. Akhmedova. Russ. J. Inorg. Chem. 2018. V. 63. № 12. P. 1617. <https://doi.org/10.1134/S0036023618120021>
- [4] D.D. Ramteke, R.S. Gedam. Solid State Ion. 2014. V. 258. P. 82. <https://doi.org/10.1016/j.ssi.2014.02.006>
- [5] A.V. Egorysheva, O.G. Ellert, Yu.V. Maksimov et al. J. Alloys Compd. 213. V. 579. P. 311. <https://doi.org/10.1016/j.jallcom.2013.06.096>
- [6] F. Berkemeier, M. S. Abouzari, G. Schmitz. Appl. Phys. Lett. 2007. V. 90. 113110. <https://doi.org/10.1063/1.2713138>
- [7] R. Korthauer (Ed.), Lithium-Ion Batteries. Basics and Applications. Springer-Verlag GmbH Germany, 2018. 415 p. <https://doi.org/10.1007/978-3-662-53071-9>
- [8] P. Knauth. Solid State Ion. 2009. V.180. P. 911. <https://doi.org/10.1016/j.ssi.2009.03.022>
- [9] Y. Duan, D.C. Sorescu. Phys. Rev. B. 2009. V. 79. № 1. P. 014301. <https://doi.org/10.1103/PhysRevB.79.014301>
- [10] M. M. Islam, T. Bredow, C. Minot. J. Phys. Chem. B. 2006. V. 110. P. 9413.
- [11] L. Liu, V.E. Henrich, W.P. Ellis, I. Shindo. Phys. Rev. B. 1996. V. 54. P. 2236.
- [12] A.B. Rahane, P.A. Murkute, M.D. Deshpande et al. J. Phys. Chem. A. 2013. V. 117. № 26. P. 5542–5550. <https://doi.org/10.1021/jp404225k>
- [13] X. Jiang, Z. Zhang, D. Luo, et al. Int. J. Quantum Chem. 2021. V. 121 Iss. 23. e26802. <https://doi.org/10.1002/qua.26802>.
- [14] G.E. Gurr, P.W. Montgomery, C.D. Knutson, B.T. Gorres. Acta Cryst. B. 1970. V. 26. P. 906.
- [15] H. Effenberger, C.L. Lengauer, E. Parthe. Monats. Chem. 2001. V. 132. P. 1515.
- [16] C.T. Prewitt, R.D. Shannon. Acta Cryst. B. 1968. V. 24. P. 869.

- [17] V.V. Maslyuk, M.M. Islam, T. Bredow. Phys. Rev. B. 2005. V. 72. P. 125101
- [18] T. Bredow, M.M. Islam. Surface Sci. 2008. V. 602. № 13. P. 2217. <https://doi.org/10.1016/j.susc.2008.04.032>
- [19] V.P. Glushko. Thermal constants of substances. Database. URL: <http://www.chem.msu.su/cgi-bin/tkv.pl?show=welcome.html>.
- [20] O. Kubaschewski, C.B. Alcock. Metallurgical Thermochemistry. 5th ed., Pergamon Press. Oxford, New York, Toronto. 1979.
- [21] I. Barin, G. Platzki. Thermochemical Data of Pure Substances. Third ed. Weinheim. VCH, New York. 1995. 1900 p.
- [22] Thermal constants of substances. Directory in ten issues / Ed. Glushko V.P. VINITI AN USSR. Moscow. 1978. Issue. 8. Part 1. 535 p. (in Russian)
- [23] S.N. Mustafaeva, M.M. Asadov, S.S. Guseinova et al. Phys. Solid State. 2022. T. 64. № 6. C. 628. <https://doi.org/10.21883/FTT.2022.06.52388.299>
- [24] M.M. Asadov, S.N. Mustafaeva, S.S. Guseinova et al. Phys. Solid State. 2021. V. 63. № 5. P. 797. <https://doi.org/10.1134/S1063783421050036>
- [25] J.P. Perdew, K. Burke, M. Ernzerhof. Phys. Rev. Lett. 1996. V. 77. № 18. P. 3865. <https://doi.org/10.1103/physrevlett.77.3865>
- [26] H.J. Monkhorst, J.D. Pack. Phys. Rev. B. 1976. V. 13. № 12. P. 5188. <https://doi.org/10.1103/physrevb.13.5188>
- [27] M.M. Asadov, S.N. Mustafaeva, S.S. Guseinova et al. Microelectronics. 2023. V. 52, № 1. C. 46. <https://doi.org/10.31857/S0544126922700181>, EDN: CXXQYI
- [28] L. Liu, V.E. Henrich, W.P. Ellis, I. Shindo. Physical Review B. 1996. V. 54. № 3. P. 2236. <https://doi.org/10.1103/PhysRevB.54.2236>
- [29] J.-J. Yeh. Atomic Calculation of Photoionization Crosssection and Asymmetry Parameters. Gordon and Breach, New Jersey, 1993.
- [30] S.P. Gordienko, B.V. Fenochka, G.Sh. Viksman. Thermodynamics of lanthanide compounds. Handbook. Kyiv: Naukovo Dumka. 1979. P. 186. (in Russian). <https://materialsproject.org/materials/mp-2652/>
- [31] M. Zinkevich. Prog. Mater. Sci. 2007. V.52. № 4. P. 597. <https://doi.org/10.1016/j.pmatsci.2006.09.002>
- [32] E.I. Suvorova, O.V. Uvarov, A.V. Ovcharov et al. Philosophical Magazine A. 2018. V. 98. № 35. P. 3127. <https://doi.org/10.1080/14786435.2018.1521013>
- [33] G. Rousse, B. Baptiste, G. Lelong. Inorg. Chem. 2014. P. 1-9. <https://doi.org/10.1021/ic500331u>